Automated Classification of Liver Cancer Stages Using Deep Learning on Histopathological Images

Velayutham Rethnagurusamy Kavitha[1], Faritha Banu Jahir Hussain[2*], Prameeladevi Chillakuru[3], Padmapriya Shanmugam[3]

[1] Department of Computer Science and Engineering, R.M.K Engineering College, Kavaraipettai 601206, India
[2] Department of Computer Science and Engineering, SRM Institute of Science and Technology, Ramapuram, Chennai 600089, India
[3] Department of Artificial Intelligence and Data Science, Velammal Institute of Technology, Ponneri 601204, India

Corresponding Author Email: farithat@srmist.edu.in

ABSTRACT

Plagued by a high incidence rate worldwide, liver cancer comes in sixth place among all cancers. The degree of differentiation, which may be roughly divided into three types: weakly moderately differentiated, highly differentiated, and differentiated, has a substantial impact on the malignancy level of this terrible illness. In direction to improve the existence of affected role and life expectancy, therapeutic techniques that are customised for these varied levels of diversity are essential. The gold standard for identifying the main liver cancer, hepatocellular carcinoma (HCC), is a histopathological picture that allows for exact distinction of liver tumours at different stages of development. This study explores the creative use of the R-CNN algorithm for deep learning for the astute categorization of histological pictures associated with liver cancer that undergoes differentiation. So this study compared how well R-CNN did compared to five other popular deep learning models - SKNet, ResNet CBAM, ResNet50, VGG16, and SENet. It was really important to set up a good system to collect a lot of different data for this project. This would make sure they had enough info to properly test how well the different math models worked. They also created a thorough and precise method using things like recall, confusion matrices, F1-scores, and accuracy to analyze how the models performed. The results showed that R-CNN did amazingly well, with an accuracy of 96.7%! That means it was able to classify things correctly almost all the time. This demonstrates it had the most accurate predictions out of everything they looked at. Additionally, the R-CNN model proved to be very reliable and able to generalize well. In other words, it should work just as good on new, unseen data as it did on the information it was originally skilled on. This study compares the routine of R-CNN to five other well-established deep learning models: SKNet, ResNet CBAM, ResNet50, VGG16, and SENet. Developing a robust data collection infrastructure is critical to enable the project to ensure a large and varied dataset for thorough evaluation of the mathematical models under consideration. A comprehensive and precise evaluation approach was provided through judicious usage of metrics like F1-Score, recall, confusion matrix, and accuracy to analyze the model performance. Testing results demonstrate R-CNN's capabilities, evidenced by its notable 96. 7% accuracy indicating highly precise classification outcomes. Furthermore, the model exhibits strong reliability and generalizability.

1. INTRODUCTION

Liver cancer carriages a significant menace to health of the human and life expectancy. Hepatocellular carcinoma (HCC), a main liver cancer originating after liver cells, is an aggressive form of cancer. Each year, approximately 905,677 original cases of liver cancer are identified globally, with an impermanence rate as high as 90 percent. Liver cancer is the third important cause of cancer death globally. In 2020 alone, over 747,000 deaths from liver cancer were reported across the globe, in addition to more than 830,120 new cases. So, China accounts for around half of the universal problem of liver cancer. Being able to identify early what stage the liver cancer is at is really important for deciding the best treatment plan going forward. The potential of these advanced algorithms for machine learning to identify malignant liver lesions at an early stage is remarkable. For people who have this kind of cancer, more rapid and successful medical therapy may be possible due to the increased detection. Overall, developing liver cancer detection tests as well as therapy options through ongoing research remains a critical globally health concern.

Understanding precise staging for cancer of the liver is crucial for creating customized therapies for each patient. The accurate data that these deep learning algorithms may offer on

the amount and spread of the disease allows for the development of customized therapies. By contrast, typical microscope assessment of samples of tissue might be personal, with varying views across clinicians about what they observed [1, 2]. The use of deep learning ushers in a new era of consistent and impartial analysis, minimizing differences in medical professionals' viewpoints and guaranteeing precise results.

Correctly identifying the stage of cancer of the liver may significantly enhance the chances of receiving optimal treatment. Doctors can employ special medications, radiation therapy, or an operation, according to the stage. Using deep learning for liver cancer staging has sped up research in medical imaging and pathology [3, 4]. This has helped doctors understand the disease better and develop modern ways to diagnose and treat it.

Catching liver cancer early and staging it precisely can save a lot of money for our healthcare system. That's because if caught late, treatments are more advanced and expensive. As deep learning keeps getting better, it will help create even more advanced models for diagnosing liver cancer stages. That will help doctors manage the disease even more.

1.1 Limitations of current diagnostic methods

Liver cancer has emerged as a formidable threat to human life and health over recent years, with both its global incidence and fatality rates on a steady incline [5-7]. The primary diagnostic methods currently employed comprise image tests, serum tests, and biopsies. Histopathological scans provide a detailed portrayal of liver cancer features, such as satellite nodules, metastases, and adjacent lesions, as well as crucial factors like the degree of differentiation, size, location, number, type, cellular, capsular, and vascular invasion.

Among these factors, the degree of differentiation significantly influences the malignancy level. The malignancy decreases as the cells become more differentiated from each other and from the normal tissue cells. Conversely, the malignancy escalates as differentiation decreases [8, 9].

Given the importance of diagnosing liver cancer with diverse degrees of differentiation, precise classification of histological images of liver cancer is both essential and irreplaceable. However, classifying histopathological images with different levels of differentiation presents challenges. It is not only time-consuming and labor-intensive, requiring substantial manual effort, but it is also prone to errors due to the subjectivity of the individual and the variable experience levels of physicians. Such misjudgements can significantly impact the formation of a patient's prognosis and treatment plan [10].

Hence, the ongoing research into the classification of liver cancer histological images carries substantial relevance and promise [11, 12].

1.2 Role of AI in medicine

In the wake of rapid advancements in artificial intelligence, the medical domain has extensively leveraged AI algorithms in recent years. Deep learning, an AI technique predicated on deep neural networks, constitutes one such artificial intelligence algorithm [13]. Computer vision and NLP tasks frequently employ deep learning, especially in the arenas of early disease diagnosis and medical image processing [14, 15].

In a significant study, Krishan and Mittal [16] utilized six distinct classifiers to categorize various tumor stages derived from CT scans. Their tumor classification accuracy spanned from 77.47% to 89.12%, thereby enabling radiologists to expedite the diagnosis and treatment of liver ailments substantially. However, this study also has limitations such as the exclusive use of one type of sample.

Xu et al. [17] proposed a radiomic diagnosis model that effectively distinguished between intrahepatic cholangiocarcinoma (ICCA) and hepatocellular carcinoma (HCC) using CT images. With AUCs (Area Under the Curve) of 0.847 in the assessment cohorts and 0.659 in the validation, this model will facilitate differentiation between ICCA and HCC in future. Nonetheless, this study underscores the need for enhanced classification accuracy.

Wan et al. [18] presented the MMF-CNN, a novel methodology that integrates multi-level and multi-scale fusion techniques within Convolutional Neural Networks (CNNs) for the purpose of detecting liver lesions in magnetic resonance imaging (MRI). They systematically used their inventive technique on several cutting-edge deep learning systems. The results of the research support the efficacy of their proposed strategy and highlight the way it may enhance the accuracy of MRI images used for assessing lesions in the liver.

Zhou et al.'s [19] comprehensive examination of machine learning (ML) and deep learning (DL) methods established a foundation for scientific literacy in the artificial intelligence (AI) field. In addition, they concentrate on convolution neural networks (CNNs) and its application to liver-related imaging issues. The real-world study in the article shows how AI can be used to detect and assess specific liver areas, enhance the results of therapy, and predict the liver's reactions to medicines. Their cooperative study supports machine-assisted health as a possible development in liver-related therapies.

In the same vein, Sureshkumar et al. [20] developed an entirely automatic Computer-Aided Diagnostic (CAD) approach for detecting hepatocellular carcinoma (HCC) employing CNN design. The present investigation has investigated a variety of techniques and algorithms used to assess cancer of the liver.

The suggested approach seeks to enhance overall precision while identifying rare tumours with a smaller rate of false positives. In addition, the study provides an original method to categorize liver scans with CT and determine between regular and unusual patterns. When put together, these findings present exciting novel perspectives as to how AI could enhance liver disease diagnosis and paving the door for better and more precise treatments.

1.3 Deep learning in liver cancer diagnosis

Due to the limitations caused forth by fewer participants, the study left the diagnosis criteria unchanged. In Lin et al.'s study [21], a Convolutional Neural Network (CNN) was carefully constructed utilizing the VGG framework. This contributed to a classification accuracy of more than 92% for all stages of liver cancer.

Using a deep learning algorithm together with multi-photon imaging demonstrated potential in differentiating between various forms of hepatocellular carcinoma (HCC), opening up fresh possibilities for automated testing [22]. There is plenty of potential for enhancement of accuracy, given that the study is still in its infancy. This work enhances the process of effectively collecting characteristics from medical visuals by incorporating a visual focus system to the deep learning

framework.

2. DATASET

The Hepatocellular Carcinoma Dataset (HCC dataset) included 165 number of 256×256 liver cancer histopathology images which were used in the present study. There are 68 histological photos with moderate differentiation, 53 images with very different images, and 44 images with weak differentiation. The HCC dataset utilized in the present research was politely provided by a Portuguese college hospital. Within-depth data on 165 actual individuals who have been identified as having hepatocellular carcinoma (HCC) could be found in this dataset. In addition to demographic details, risk factors, outcomes of tests, and a wealth of data related to longevity, the dataset contains every necessary medical data. This rich and diverse dataset serves as a valuable resource for conducting a thorough and insightful analysis of HCC, enabling researchers to glean meaningful insights into the various factors associated with this disease in a real-world clinical setting.

The dataset includes 49 features that were chosen in accordance with the EASL-EORTC Clinical Practice Guidelines, which represent the most recent advances in the treatment of HCC and the dataset is available in https://archive.ics.uci.edu/dataset/423/hcc+survival.

3. MATERIALS AND METHODS

Figure 1 shows the architecture diagram. Initially input image is taken from the Kaggle Dataset and pre-processed with Weiner filter then segmented and extracted features using FCM-CSA and SIFT algorithms respectively. Extracted features are classified using R-CNN and liver tumor is classified with different classes. This classification helps the medical experts to take the right decisions at right time to save the human life. Gray-Level Co-occurrence Matrix (GLCM) can be a valuable tool for feature extraction in liver cancer identification, especially when analyzing medical images like CT scans, MRIs, or ultrasound images for texture analysis, discriminative features, local analysis and interpretability. For liver cancer identification need to features are very important for classification so only GLCM was utilized in the proposed work.
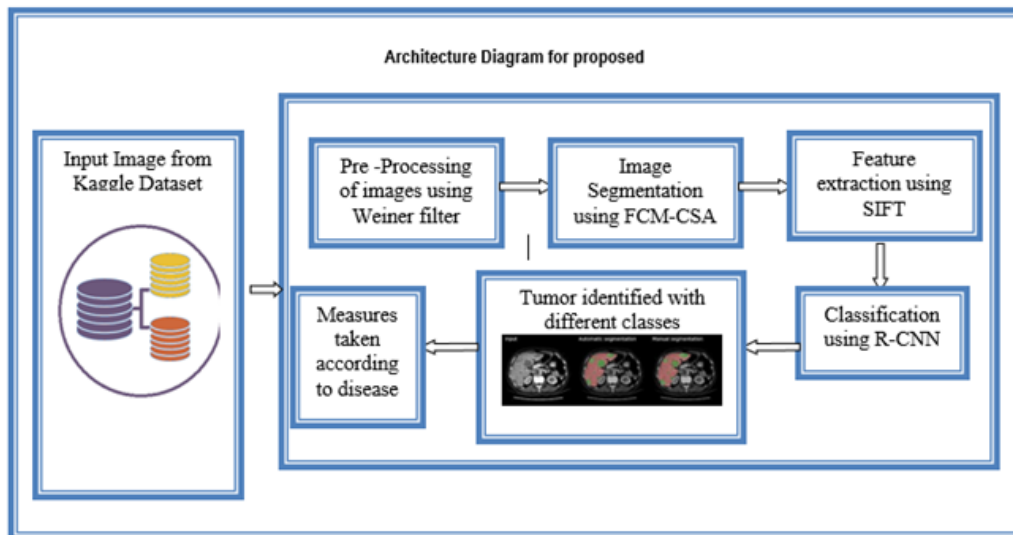

Figure 1. Architecture diagram for proposed method

R-CNN (Region-based CNN) is powerful computer vision techniques that have been widely used in various applications, including object detection, image segmentation, and more. While these techniques are not specific to liver cancer identification and classification, they can be essential tools in the field of medical image analysis, including liver cancer identification and classification, for several reasons like accurate detection, localization, feature classification, and extraction.

While R-CNN and its variants offers many advantages, it's significant to note the success be contingent on the availability of high-quality annotated medical image datasets and the expertise of healthcare professionals to interpret the results and make informed decisions based on the model's predictions.

3.1 Image pre-processing

The foundational step is pre-processing, a crucial stage in which input images are sourced from both the Kaggle dataset and on-site field visits. During pre-processing, the objective is to eliminate undesirable noise from the images while simultaneously boosting the contrast levels to enhance overall image quality.

In liver cancer identification and classification, pre-processing prepares the raw medical images for subsequent feature extraction and AI based algorithms. It ensures that the data used for analysis is accurate, consistent, and conducive to reliable results, ultimately improving the diagnostic and classification accuracy for liver cancer.

Figure 2 (a) shows input image of Histopathological image of liver with Cancer and Figure 2 (b) shows the pre-processed image of liver with cancer cells.

3.2 Segmentation using Fuzzy C-Means (FCM)

In the segmentation of diseased (cancerous) portions, an innovative approach called FCM-CSA (Fuzzy C-Means based Chameleon Swarm Algorithm) was applied. The segmentation

process within FCM-CSA is delineated through the following steps: Leveraging the principles of fuzzy logic, an unsupervised classification model akin to the Fuzzy C-Means (FCM) network was introduced. Unlike traditional partitioning models such as k-means, where each data point corresponds to a single partition, the FCM model allows for a more nuanced representation of data points within multiple partitions, providing a richer and more flexible segmentation framework.
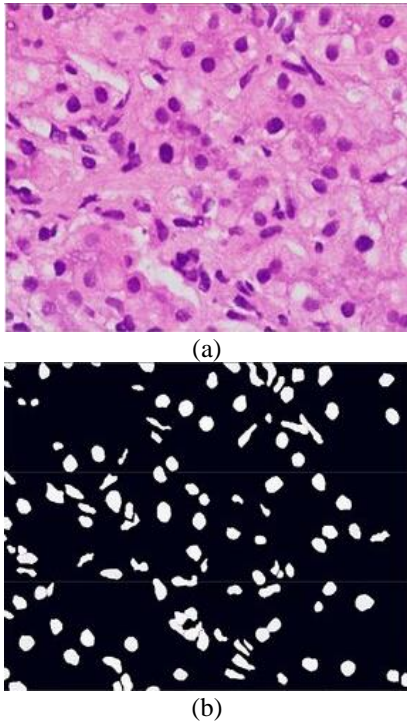

(a)

(b)

Figure 2. a) Histopathological image of liver with cancer b) Pre-processed liver with cancer

Eq. (1) calculates the cluster centers:

$$Dj = \frac{\sum_{K=1}^{M} V_{j,k}^{n}{}_{Y_k}}{\sum_{K=1}^{M} V_{j,k}^{n}} \qquad (1)$$

The dataset comprises M data points, denoted as y_k, where k represents the index of each pixel. The degree of membership for the kth pixel is expressed through a fuzzifier denoted as 'n,' with the constraint that 'n' is greater than 1. Eq. (2) articulates the formula that encapsulates this relationship, providing a mathematical representation of the degree of membership for each pixel in the dataset.

$$V_{j,k} = \frac{1}{\sum_{L=1}^{md} \frac{C_{j,k}^{2/(n-1)}}{C_{j,k}}} \qquad (2)$$

Degree of membership is represented by v(j,k). c2(yk, dj) gives the distance that exists between the jth group and the kth pixel. The parameter 'n', which provides a fuzziness level where $1 < n \leq \infty$, plays an essential part when determining the number of membership degrees. The method described in look at 1 yields ideal clustering centers, which can be utilized to help segment the malignant disease off the image.

The Fuzzy C-Means (FCM) method has certain issues throughout the segmentation process, particularly with the initial cluster centroids' poor performance. In order to accomplish this, we employ a mixed approach that involves the FCM-based Chameleon Swarm Algorithm (CSA), additionally referred to as FCMCSA. The meta-heuristic technique known as the CSA begins the optimization procedure with initializing the number of participants. The first population is formed with a random initialization in a search space, assuming an overall population count of 'C' within the search space of size 'D'. By utilizing the benefits of both FCM and CSA, this combination approach reduces the limitations of FCM's original cluster centroids and enhances segmentation quality overall.

$$a_i = L_j + rand \times (U_j - L_j) \qquad (3)$$

The first vector of ith chameleon is represented by a_i, with the upper and lower limits of the search area defined as L_j and U_j in the jth dimension, respectively. The variable rand denotes a randomly generated number within the range of 0 to 1. The reinforced exploratory capabilities of the chameleons in the search space are succinctly articulated as follows:

$$\rho = \delta \, exp^{(-\frac{\alpha t}{R})} \qquad (4)$$

In the iterative process, the parameter ρ plays a pivotal role and diminishes as the iterations progress. Predefined parameters δ, α, and β are strategically employed to govern the delicate balance between exploration and exploitation stages. The updating of chameleons' positions in the search space is orchestrated through rotating centered coordinates, coupled with an acceleration factor. With Figure 3 offering a representation of the input image alongside the segmented output achieved through the FCM-CSA.
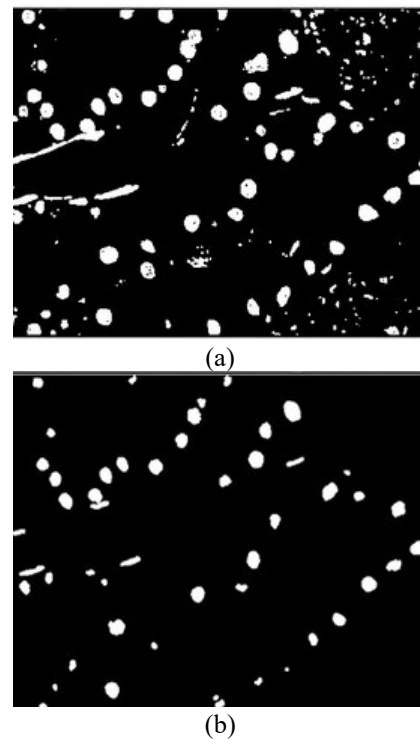

(a)

(b)

Figure 3. a. Binary image; b. Segmented image using FCM-CSA algorithm

3.3 Feature extraction using GLCM

Following segmentation, the next step involves feature extraction through a rapid GLCM (Gray Level Co-occurrence Matrix) feature extraction model. Typically, GLCM features provide comprehensive texture descriptions of images, but their computational intensity poses a significant resource challenge. In this model, the gray levels of image pixels undergo re-quantization to minimize G, enhancing the efficiency of the GLCM feature extraction process. The fast GLCM model proves to be a robust method for extracting features related to liver cancer disease. The model operates by establishing connections between spatially close pixel features, calculating GLCM matrices under the correlation type, and assigning index pixels to all pyramid weight matrix neighborhoods. To estimate GLCM features for other pixels, this model, as illustrated in Eq. (5), is employed, ensuring a comprehensive and efficient extraction process.

$$F(q) = \sum_{j=1}^{m} bj\,(q)F(yi) \qquad (5)$$

The feature vector for non-key pixels, denoted as $F(q)$, is defined, with each overlapping weight window centered on a key pixel equal to y_j. To assess the efficacy of the fast GLCM performance, simulations are conducted with varied image sizes, utilizing three single-band images for validation. The simulation employs the following parameters, and the results are visually depicted in Figure 4, showcasing the extracted features from a histopathological image depicting liver cancer using GLCM.

Figure 4. Feature extraction using GLCM

- Utilizing a fixed window size of 33 × 33 for GLCM extraction simplifies the process. The extracted features using the GLCM algorithm are illustrated in Figure 4.
- The execution load of GLCM is effectively reduced, and sparsity of GLCM matrices is reduced through strategic adjustments.
- To diminish the computational load (G), a re-quantization of the input image gray levels is performed.

3.4 Feature classification using fast R-CNN

A powerful object detection tool, known as the Fast Region-Based CNN (Fast R-CNN), employs deep learning techniques for categorizing objects within an image. Leveraging the Edge Boxes approach, it enhances the computational efficiency of object detection by generating effective region proposals.

Edge Boxes provide a straightforward measure of objectness, subtracting edges that are part of contours crossing the border of the box's.

Possible object-containing areas are initially meticulously delineated using Edge Boxes in the two-stage Fast R-CNN recognition technique. In the next phase, each component is classified. In the first step, layers of convolution are employed to analyze the entire picture with the goal to extract features. In addition to generate region ideas and extract characteristics from the image, Edge Box are additionally processed at this stage.

Regions of interest (ROIs) in hepatic pictures are identified and categorized via Fast R-CNN, which finds application to liver cancer classification. The assessment of Fast R-CNN's performance in detecting liver cancer can be performed using a number of criteria, such as precision, recall, precision, accuracy, and F1-Score. The device's operating characteristic curve's area under the curve (AUC-ROC).

Accuracy calculates the precision of positive diagnoses among every sample marked as positive, while accuracy estimates the proportion of properly classified samples. Among every one of the genuine positive samples, recall assesses the precision with which positive classification have been generated. Recall and accuracy are evaluated in an equitable way by the F1 score. The ability of the model to differentiate between samples that are positive or negative across a range of threshold is assessed with AUC-ROC.

A set of annotated liver images that can tell the difference among malignant or non-cancerous material is essential to evaluate the efficacy of Fast R-CNN in cancer of the liver diagnosis. Three sets of data points have been divided into test, validation, and learning. The model changes on its initial set throughout training, changing hyperparameters for learning rate and batch count for optimal. These evaluations help identify the model's benefits and drawbacks, directing potential enhancements to the layout and training methods. Three different categories utilizing the Fast R-CNN technique are shown visually in Figure 5.
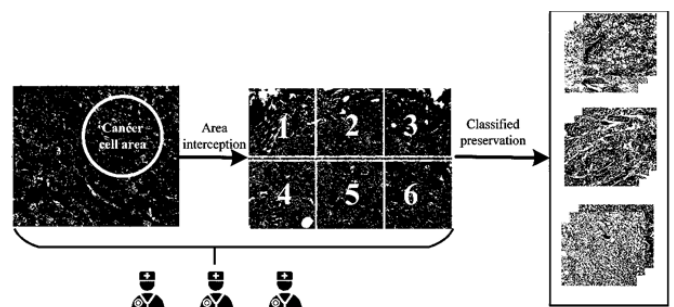

Figure 5. Different classes of classification using R-CNN algorithm

3.4.1 Training

By utilizing an image the labeler is an essential for object detectors training such as Fast R-CNN. The image labeler program facilitates the assignment of predetermined rectangular Regions of Interest (ROIs) labels to a set of photographs, distinguishing them into three types: poorly differentiated, well differentiated, and moderately differentiated. During the training process, expert doctors are actively involved in classifying liver cancer from low to high grades.

The labeled ROIs for each image can be exported to the MATLAB workspace. After creating ROIs and labels for each image in a collection, a command like "trainingData" can be used. This exported ground truth serves as crucial input during the training phase.

The object detector introduced in this model; Fast R-CNN is built upon the foundation of the VGG-16 Convolutional Neural Network (ConvNet). The VGG-16 ConvNet undergoes a transfer learning approach, adapting pre-trained weights for effective object detection. Each image requires a corresponding label identifying the rectangle region of interest (ROI). In this study, the region for each image in its label column is set to [1, 1, 224, 224], given that every image in the dataset is a cropped image of liver cancer.

Modifications to the VGG-16 model include adjusting the dimensions of the last three layers and the image input layer from [224, 224, 3] to [48, 48, 3]. Additionally, the grayscale picture dataset undergoes transformation from [48, 48, 1] to [48, 48, 3]. Further enhancements involve the addition of a region-of-interest pooling layer and a bounding box regression layer, transforming the pre-trained model into Fast R-CNN object identification network. This adaptation ensures the effective integration of the VGG-16 model into the Fast R-CNN framework for accurate liver cancer classification.

4. EXPERIMENTAL RESULT ANALYSIS

Three key parameters—specificity, accuracy, and recall— as indicated in Eqs. (6)-(8) are all taken into consideration in assessing the effectiveness of the planned work. These indicators serve as crucial criteria for evaluation, providing an in-depth understanding of the effectiveness of the strategy. True negative (TN), false positive (FP), false-negative (FN), and true positive (TP) among others, were the four unique parameters which make up the evaluation [23, 24].

$$Precision = \frac{TP}{FP + TP} \qquad (6)$$

$$SP = \frac{TN}{TN + FP} \qquad (7)$$

$$recall = TP / TP + FN \qquad (8)$$

The figures that are given provide strong proof of the enhanced efficacy of the suggested strategy, showing high Precision, Recall, and Specificity scores. Consequently, the R-CNN model achieved a remarkable 97.27% final accuracy. The R-CNN neural network model's effectiveness in the smart classification of images from histopathology is demonstrated by this study.

In this framework, an original comparative analysis has been carried out, where four different innovative deep learning models—ResNet50 CBAM, ResNet50 SKNet, VGG16, and SEnet—were contrasted with the R-CNN deep training model. Notably, it's the initial occasion that comparison this comprehensive was made in an intelligence categorization study of pictures reflecting multiple kinds of differentiating tumors of the liver histology, or the findings illustrate the efficiency of the R-CNN model in exceeding its rivals and establish it as an effective tool for cognitive histopathology image classification.

A significant development in the discipline of histopathology categorization of images was made possible by the R-CNN's exceptional 97.27% precision in classification. This study clearly indicate that the R-CNN deep learning algorithm has a lot of possibilities for correctly identifying photos related to histopathology. This development is especially helpful for physicians since it enables more efficient planning of therapy according to each phase of cancer, which in turn ensures prompt and specialized patient care. R-CNN installation can both lessen the quantity of labor that doctors have to do as cut back on the length of time needed for interpreting cancer of the liver histopathology images.

Figure 6 provides an illustration of the analysis's findings enabling simple comprehension. In addition, Table 1 offers an in-depth contrast between the suggested Fast R-CNN approach and the performance of renowned liver cancer classification algorithms, like SVM, RETRaiN, SBN-CNN, VGG-19, and CB-CNN [24, 25]. The table further delves into a detailed comparison of precision, emphasizing the correct identification of objects. In this evaluation, the proposed method is pitted against existing algorithms SVM, RETRaiN, SBN-CNN, VGG-19, and CB-CNN [26], highlighting its effectiveness in the classification recognition domain.

The confusion matrix, a crucial tool for elucidating various metrics, is visually presented in Figure 7 and detailed in Table 2. In this matrix, the predicted labels are indicated in rows, while the original labels are presented in columns, categorizing liver tumors into benign and malignant states. The matrix distinctly illustrates the performance of the proposed R-CNN method, showcasing its superior classification capabilities.

In the context of liver cancer classification with the R-CNN algorithm, the confusion matrix enables an assessment of how well the algorithm classifies different types of liver cancer. In this example, rows represent expected classes, and columns indicate actual classes. Each cell indicates the number of instances where the expected class aligns with the actual class.

Table 1. Precision, recall and specificity of the proposed method fast R-CNN

Algorithm	Precision	Recall	Specificity
SVM	0.807	0.818	0.917
SBN-CNN	0.802	0.883	0.937
RETRaiN	0.781	0.871	0.918
CB-CNN	0.805	0.836	0.927
VGG-19	0.788	0.835	0.975
R-CNN (Proposed)	0.898	0.891	0.952

Table 2. Confusion matrix

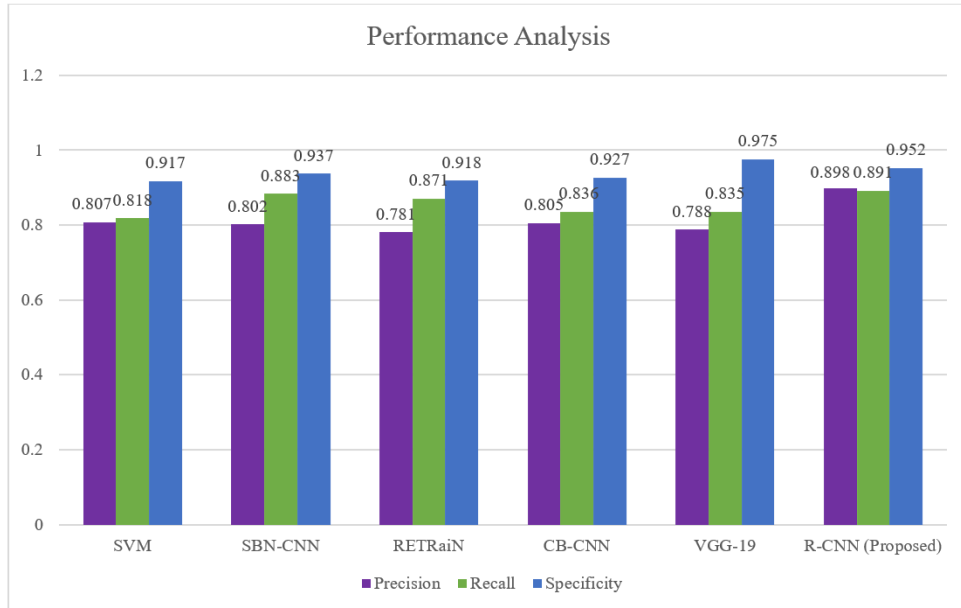|	Actual Hepatocellular Carcinoma	Actual Cholangiocarcinoma	Actual Metastatic Carcinoma
Predicted Hepatocellular Carcinoma	50	10	5
Predicted Cholangiocarcinoma	5	30	8
Predicted Metastatic Carcinoma	2	8	40

Figure 6. Performance Analysis of proposed algorithm (precision, recall and specificity)
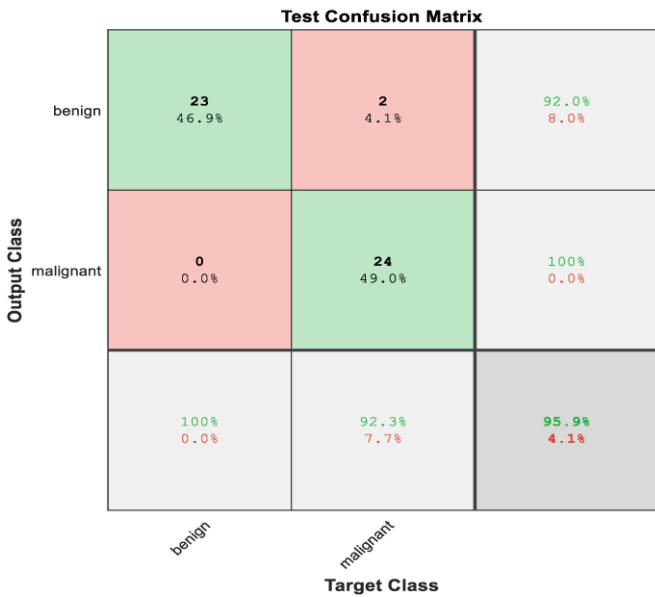

Figure 7. Confusion matrix

To interpret this matrix, you can calculate various evaluation metrics such as precision, recall, and F1-score. For instance, the precision for predicting Hepatocellular carcinoma would be calculated as TP/(TP + FP) = 120 / (120 + 15) = 0.889, where TP is the number of true positives (correctly predicted Hepatocellular carcinoma), and FP is the number of false positives (predicted as Hepatocellular carcinoma, but actually a different type of liver cancer). This analysis helps provide a nuanced understanding of the algorithm's performance in liver cancer classification.

The HCC datasets employed in this study have been meticulously partitioned into distinct sets for comprehensive training, validation, and evaluation of the proposed model. To be more exact, 90% of the data has been set aside for learning, 7% for validation, then 3% for extensive testing. This intentional divide ensures the model's generalization and resiliency.

The proposed model has been trained and refined with the first two sets of data, which total 90% of the training data and 7% for validation. This allows the model to grow comfortable with the subtleties of the HCC dataset. The test data set, making up 3% of the initial data set, will be utilized only to assess the extent to which the suggested approach detects items. To enhance clarity, Table 3 provides an overview of the image distribution between the initial training, examination, and validation sets, highlighting the volume of data utilized in every phase of the research. This meticulous arrangement ensures a stringent examination and testing procedure for the provided model, increasing the model's reliability and adaptability for determining cancer of the liver.

Table 3. Usage of images for training and testing

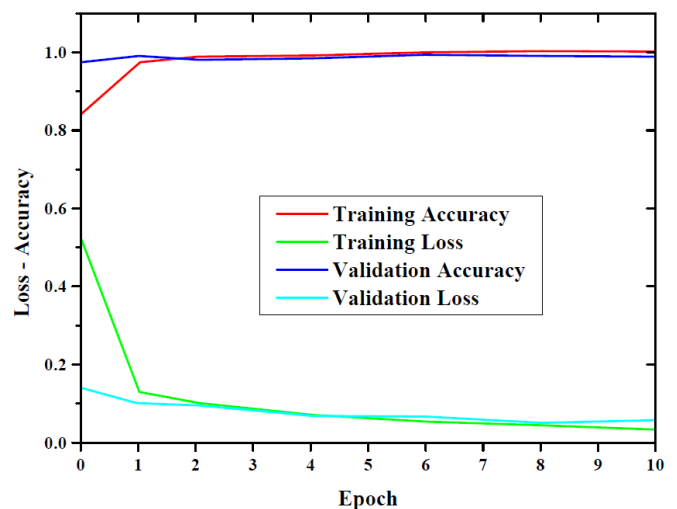|	Training	Testing	Validation	Total
HCC Image Dataset	148 (90%)	12 (7%)	5 (3%)	165

Figure 8. Convergence curves for validation and training datasets

The suggested Fast R-CNN model's efficacy appears on the chart in Figure 8. The red and dark blue lines for correctness reflect the training and verification curves, while the green and

sky-blue lines represent the training and validation loss. surprisingly, the loss curve increases rapidly in the initial two epochs until it finally settles around the seventh one epoch. The validation and training curves gradually align that look at confluence after a few additional training epochs as the algorithm improves.

5. CONCLUSION

In short, the region-based convolutional neural networks (RNCNN) and Fuzzy C-Means (FCM) algorithms exhibit potential in identifying signs of cancers of the liver from clinical images. R-CNN shows efficiency in recognizing and classifying areas of interest (ROIs) in liver images, allowing doctors determine malignant regions and renders liver cancer detection and therapy easier. Together with each other, the outcome measures provide an in-depth comprehension of the R-CNN model's capacity to identify and categorize pertinent regions in liver images, which is crucial to enhancing the accuracy and efficacy of liver cancer diagnosis and therapy planning. However, FCM is a useful technique for clustering that can help identify trends and links between the image pixels for purposes of diagnosing liver cancer. Each pixel in FCM may be given a degree for membership which reflects its likelihood of slipping into a particular category (cancerous or non-cancerous). Metrics like cluster purity, entropy, and precision can be used to evaluate the efficacy of FCM. When comparing the two techniques, R-CNN could prove more accurate and reliable at recognizing and categorizing ROIs in liver pictures, while FCM could provide an easier to use analysis of the image's features or aid in determining the location of the liver's regions. The suggested approach goes above the current methods utilized in this field of study for performance contrast, attaining accuracy of 0.898, recall of 0.891, and a sensitivity of 0.952. R-CNN and its variants can be computationally demanding, especially during the training phase. Training deep neural networks on medical image datasets, which are often large and high-dimensional, can require significant computational resources and time. There are several potential future enhancements for deep learning-based liver cancer classification incorporating multi-modal data, Data augmentation, Transfer learning, Explainable AI, Online learning. Based on the application and size of the data set the future researcher may select LSTM, U-NET, CapsNET, and 3D-CNN.

REFERENCES

[1] Zheng, Y., Zhang, W., Xu, L., Zhou, H., Yuan, M., Xu, H. (2022). Recent progress in understanding the action of natural compounds at novel therapeutic drug targets for the treatment of liver cancer. Frontiers in Oncology, 11: 795548. https://doi.org/10.3389/fonc.2021.795548

[2] Jemal, A., Bray, F., Center, M., Ferlay, J., Ward, E., Forman, D. (2011). Global cancer statistics. CA: A Cancer Journal for Clinicians, 61(2): 69-90. https://doi.org/10.3322/caac.20107

[3] Jemal, A., Bray, F., Center, M.M., Ferlay, J., Ward, E., Forman, D. (2011). Global cancer statistics. CA: A Cancer Journal for Clinicians, 61(2): 69-90. https://doi.org/10.3322/caac.20107

[4] Sun, B., Karin, M. (2012). Obesity, inflammation, and liver cancer. Journal of Hepatology, 56(3): 704-713. https://doi.org/10.1016/j.jhep.2011.09.020

[5] Ali, L., Wajahat, I., Amiri Golilarz, N., Keshtkar, F., Bukhari, S.A.C. (2021). LDA–GA–SVM: Improved hepatocellular carcinoma prediction through dimensionality reduction and genetically optimized support vector machine. Neural Computing and Applications, 33: 2783-2792. https://doi.org/10.1007/s00521-020-05157-2

[6] Sheng, D., Xu, F., Yu, Q., Fang, T., Xia, J., Li, S., Wang, X. (2015). A study of structural differences between liver cancer cells and normal liver cells using FTIR spectroscopy. Journal of Molecular Structure, 1099: 18-23. https://doi.org/10.1016/j.molstruc.2015.05.054

[7] Bray, F., Ferlay, J., Soerjomataram, I., Siegel, R.L., Torre, L.A., Jemal, A. (2018). Global cancer statistics 2018: GLOBOCAN estimates of incidence and mortality worldwide for 36 cancers in 185 countries. CA-Cancer J Clin., 68(6): 394-424. https://doi.org/10.3322/caac.21492

[8] Liao, H., Xiong, T., Peng, J., Xu, L., Liao, M., Zhang, Z., Zeng, Y. (2020). Classification and prognosis prediction from histopathological images of hepatocellular carcinoma by a fully automated pipeline based on machine learning. Annals of Surgical Oncology, 27: 2359-2369. https://doi.org/10.1245/s10434-019-08190-1

[9] Sun, C., Wang, Y.X., Sun, M., Zou, Y., Zhang, C., Cheng, S., Hu, W. (2020). Facile and cost-effective liver cancer diagnosis by water-gated organic field-effect transistors. Biosensors and Bioelectronics, 164: 112251. https://doi.org/10.1016/j.bios.2020.112251

[10] Khan, M.A., Rubab, S., Kashif, A., Sharif, M.I., Muhammad, N., Shah, J.H., Zhang, Y.D., Satapathy, S.C. (2020). Lungs cancer classification from CT images: An integrated design of contrast based classical features fusion and selection. Pattern Recognition Letters, 129: 77-85. https://doi.org/10.1016/j.patrec.2019.11.014

[11] Xia, B., Jiang, H., Liu, H., Yi, D. (2016). A novel hepatocellular carcinoma image classification method based on voting ranking random forests. Computational and Mathematical Methods in Medicine, 2016. https://doi.org/10.1155/2016/2628463

[12] Barone, M., Di Leo, A., Sabbà, C., Mazzocca, A. (2020). The perplexity of targeting genetic alterations in hepatocellular carcinoma. Medical Oncology, 37: 1-5. https://doi.org/10.1007/s12032-020-01392-8

[13] Afza, F., Sharif, M., Khan, M.A., Tariq, U., Yong, H.S., Cha, J. (2022). Multiclass skin lesion classification using hybrid deep features selection and extreme learning machine. Sensors, 22(3): 799. https://doi.org/10.3390/s22030799

[14] Bibi, A., Khan, M.A., Javed, M.Y., Tariq, U., Kang, B.G., Nam, Y., Mostafa, R.R., Sakr, R.H. (2022). Skin lesion segmentation and classification using conventional and deep learning based framework. Computers, Materials & Continua, 71(2): 2477-2495. https://doi.org/10.32604/cmc.2022.018917

[15] Attique Khan, M., Sharif, M., Akram, T., Kadry, S., Hsu, C.H. (2022). A two-stream deep neural network-based intelligent system for complex skin cancer types classification. International Journal of Intelligent Systems, 37(12): 10621-10649. https://doi.org/10.1002/int.22691

[16] Krishan, A., Mittal, D. (2021). Ensembled liver cancer

detection and classification using CT images. Proceedings of the Institution of Mechanical Engineers, Part H: Journal of Engineering in Medicine, 235(2): 232-244. https://doi.org/10.1177/0954411920971888

[17] Xu, X., Mao, Y., Tang, Y., Liu, Y., Xue, C., Yue, Q., Liu, Q., Wang, J., Yin, Y. (2022). Classification of hepatocellular carcinoma and intrahepatic cholangiocarcinoma based on radiomic analysis. Computational and Mathematical Methods in Medicine, Article ID: 5334095. https://doi.org/10.1155/2022/5334095

[18] Wan, Y., Zheng, Z., Liu, R., Zhu, Z., Zhou, H., Zhang, X., Boumaraf, S. (2021). A multi-scale and multi-level fusion approach for deep learning-based liver lesion diagnosis in magnetic resonance images with visual explanation. Life, 11(6): 582. https://doi.org/10.3390/life11060582

[19] Zhou, L.Q., Wang, J.Y., Yu, S.Y., Wu, G.G., Wei, Q., Deng, Y.B., Wu, X.L., Cui, X.W., Dietrich, C.F. (2019). Artificial intelligence in medical imaging of the liver. World Journal of Gastroenterology, 25(6): 672-682. https://doi.org/10.3748/wjg.v25.i6.672

[20] Sureshkumar, V., Chandrasekar, V., Venkatesan, R., Prasad, R.K. (2021). Improved performance accuracy in detecting tumor in liver using deep learning techniques. Journal of Ambient Intelligence and Humanized Computing, 12(6): 5763-5770. https://doi.org/10.1007/s12652-020-02107-7

[21] Lin, H.X., Wei, C., Wang, G.X., Chen, H., Lin, L.S., Ni, M., Chen, J.X., Zhuo, S.M. (2019). Automated classification of hepatocellular carcinoma differentiation using multiphoton microscopy and deep learning. Journal of Biophotonics, 12(7): e201800435. https://doi.org/10.1002/jbio.201800435

[22] Lee, C.C., Huang, S.S., Shih, C.Y. (2010). Facial affect recognition using regularized discriminant analysis-based algorithms. EURASIP Journal on Advances in Signal Processing, 2010: 1-10. https://doi.org/10.1155/2010/596842

[23] Lekshmi, P.V., Sasikumar, M. (2009). Analysis of facial expression using Gabor and SVM. International Journal of Recent Trends in Engineering, 1(2): 47.

[24] Londhe, R., Pawar, V. (2012). Facial expression recognition based on affine moment invariants. International Journal of Computer Science Issues (IJCSI), 9(6): 388.

[25] Ma, L., Khorasani, K. (2004). Facial expression recognition using constructive feedforward neural networks. IEEE Transactions on Systems, Man, and Cybernetics, Part B (Cybernetics), 34(3): 1588-1595. https://doi.org/10.1109/TSMCB.2004.825930

[26] Umamageswari, A., Deepa, S., Raja, K. (2022). An enhanced approach for leaf disease identification and classification using deep learning techniques. Measurement: Sensors, 24: 100568. https://doi.org/10.1016/j.measen.2022.100568